Surface Electronic Structure

Regina Ragan
The Henry Samueli School of Engineering, Chemical Engineering and Materials Science
University of California, Irvine, Irvine, CA, USA

Synonyms

Local density of states

Definition

Surface electronic structure is defined by filled and empty electronic states of the system near the surface of a solid material. In both bulk systems and nanosystems, the type of atoms in the system, the atomic arrangement, and atomic order versus disorder influence electronic structure. Tight Binding, an early method for calculating electronic structure using a single particle Hamiltonian, approximates the electronic wave functions in a crystal as a linear combination of the atomic wave functions of constituent atoms. Tight Binding analysis shows that electrons in solid materials exhibit collective behavior that deviates from discrete electronic states in isolated atoms. Coupling of atomic wave functions in crystals leads to a continuum of energy states, called energy bands. The electronic structure at the surface often differs from that in the bulk due to broken bonds and atomic surface reconstructions. If the surface to volume ratio is high, as in nanosystems, then surface effects can dominate observed electronic properties.

An important physical parameter to characterize electronic structure is the Fermi energy. The Fermi energy is often referred to as the highest occupied energy state since the probability of electron occupation of states having higher energy than the Fermi energy decays exponentially at equilibrium as determined from the Fermi-Dirac distribution function. The Fermi energy level is typically measured indirectly by the work function of the material. The work function is the energy needed to remove an electron from a material and is equal to the difference between the Fermi energy and the vacuum energy level. The position of the Fermi energy with respect to the energy bands determines whether the material is a metal, semiconductor, or insulator. Consider a simplified intuitive view. If atoms in the crystal have an odd number of valence electrons, then the energy bands that arise due to splitting of atomic energy levels are half filled. In this case, as found in metals, there is a continuum of available electronic states near the Fermi energy. A low resistance to electron motion is exhibited and thus metals are good conductors. In comparison, from this simple view, if there is an even number of valence electrons in constituent atoms of the crystal, then the (valence) energy bands are completely filled at zero Kelvin and the Fermi energy is in the energy bandgap. Near zero Kelvin, in both semiconductors and insulators, electrons do not occupy states in the conduction band and thus will exhibit negligible conductivity. Near room temperature, semiconductors have few electrons at energy levels available for conduction.

In the case of nanosystems, the number of atoms in the system also affects electronic structure due to quantum confinement of electrons. In metals the "space"an electron occupies in the crystal is defined by the Fermi wavelength that has an inverse relationship with the electron density. In semiconductors, where charge carriers are electron and holes, the Bohr exciton radius defines the "space" for an electron hole pair. The Bohr exciton radius is a function of the dielectric constant of the material and the effective mass of the charge carriers. It is typically much larger than the Fermi wavelength in magnitude. When dimensions of nanoscale systems decrease below the Fermi wavelength (metals) or Bohr exciton radius (semiconductors) unique physical properties not observed in bulk materials arise due to quantum-size effects.

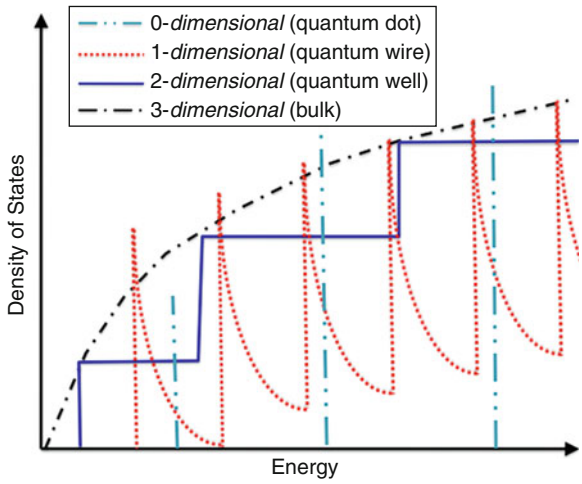

Surface Electronic Structure, Fig. 1 Schematic of density of states for 3-dimensional, bulk system (*black dot-dashed curve*), 2-dimensional, quantum well (*blue solid curve*), 1-dimensional, quantum wire (*red dashed curve*), 0-dimensional, quantum dot (*cyan double dot- dashed curve*)

Overview

Drude theory provides a simple, intuitive analysis of the collective behavior of electrons in metallic systems. After J.J. Thompson discovered the electron in 1897, Drude treated valence electrons in metals as an electron gas and applied the kinetic theory of gases to describe electrical and thermal conductivity in metals. In this model, valence electrons are assumed to move freely in the solid and the potential exerted on electrons in the crystal lattice is assumed to be uniform due to nondirectional bonding of atoms in the crystal (metals have high coordination numbers). Electrons are only assumed to interact with ion cores during finite scattering events. Thus, the model is called the free electron model and the approximation for finite scattering events is called the relaxation time approximation. Although Drude theory only works well for alkali metals, it provides a qualitative understanding of thermal and electrical conductivity in metals. Early on Sommerfeld addressed some of the shortcomings of Drude theory to evaluate thermal conductivity by using Fermi-Dirac statistics to model the velocity distributions of electrons in metals in the context of Drude theory. Quantum mechanical corrections are needed to accurately estimate the number of electrons that contribute to conductivity in most metals. Despite the need for these corrections, the approach of the electron gas to model observed electrical, thermal, and optical properties in materials was pivotal in our understanding of experimental observations in metals and semiconductors. The density of states, that is the number of available states per unit energy at a particular energy level, is derived from the electron gas approach. A schematic of how the density of states varies between bulk systems and quantum-confined systems is shown in Fig. 1. Van Hove singularities (discontinuity in the density of states) can be seen in quantum-confined systems. The concept of an electron gas is still used and describes quantum-confined systems such as metallic, single-walled carbon nanotubes (*one-dimensional* electron gas) that exhibit Van Hove singularities [1] and graphene (*two-dimensional* electron gas) that exhibits the quantum hall effect where the Hall conductivity exhibits quantized values [2].

When analyzing systems of atoms that do not form metallic bonds, ionic, and covalent systems, the approximations that bonding is nondirectional and the potential is uniform is no longer valid. Kronig and Penny provided early intuition of energy levels and bands in crystals using both Bloch's theorem and a simple one-dimensional, periodic square wave potential that roughly approximates the potential of atoms in a periodic crystalline system. Via this simple analysis it is found that there are energy levels that yield nonphysical solutions for the electron wave functions and thus are not allowed for electrons in the system. These forbidden energy levels are defined as an energy

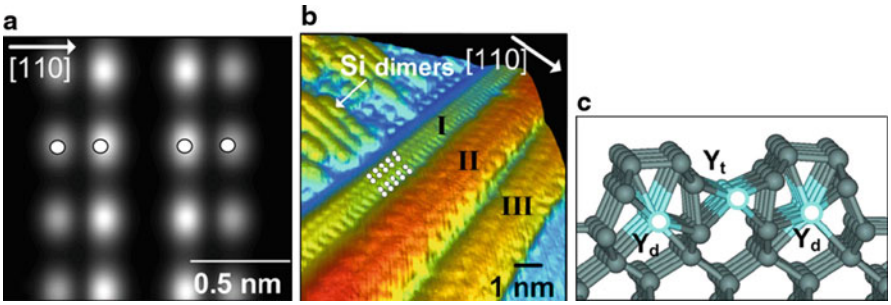

Surface Electronic Structure, Fig. 2 (**a**) DFT simulation of the calculated electronic structure on the surface of an yttrium disilicide nanowire having a width of 1.1 nm. (**b**) STM image of dysprosium disilicide nanowires on Si(001) substrate. Nanowire labeled I has a width of 1.1 nm, the calculated surface electronic structure matches the STM image as indicated by the white round circles. (**c**) Cross-sectional view of the relaxed atomic struture in the disilicide nanowires determined from DFT calculations and STM images (Printed with permission from Ref. [4])

bandgap. If the Fermi energy is in the bandgap, there are few electrons occupying energy states in the conduction band (above the Fermi energy) and thus conductivity is lower than in metals, hence the name semiconductor. As mentioned prior, the main difference between metals and semiconductors/insulators is that the Fermi energy sits within a band in a metal and in the energy bandgap in a semiconductor/insulator. The main difference between semiconductors and insulators is the magnitude of the bandgap. If greater than approximately 4 eV, then the probability of electrons occupying states in the conduction band is negligible at room temperature.

Basic Methodology

Computational Approaches

Significant advances in computational abilities coupled with important fundamental physical simplifications have allowed for first principles, ab initio, calculations of electronic structures of many body systems more closely modeling solid macroscopic and nanosystems and thus increasing accuracy. Since the Schrodinger equation cannot be solved analytically for these many electron systems, it was pivotal that Hohenberg and Kohn proved that the ground state energy of a many body system is a unique function of the charge density distribution [3]. Charge density distributions have a relationship with the atomic structure and periodicity in the crystal and thus can be evaluated by the types of atoms in the crystal and the crystal structure (atomic arrangement). Later, using an exchange correlation potential acquired from the theory of a homogeneous electron gas, Kohn and Sham determined how a many body system could be reduced to a single particle equation for input into the Schrodinger equation. This is referred to as the local density approximation [3].

Due to these critical advances in understanding of many body systems, density functional theory (DFT) is widely used to calculate electronic structure that can be directly compared to experimental systems for understanding of experimental observations or used to predict physical properties to guide experiments. For example, DFT provided fundamental understanding of low-dimensional magnetism such as giant magnetic moments found in two-dimensional systems, such as monolayers of Mn and Cr. Giant magnetic moments arise due to an increase in the density of electronic states near the Fermi energy [3]. The phenomenon of Giant Magnetoresistance allowed for an increase in storage density in magnetic hard disk drives. Furthermore, low-dimensional metallic nanowires and nanoparticles can exhibit ballistic transport or unique chemical activity, respectively, and typically require feature sizes smaller than achievable with lithography. Thus self-organization is needed for fabrication. Atomic arrangements and driving forces for self-organization of low-dimensional metallic systems can be determined using atomic scale imaging in conjunction with DFT [4, 5]. Figure 2 shows how the correlation between DFT simulations and scanning tunneling microscopy (STM) measurements allowed for an understanding of the atomic structure in disilicide nanowires that exhibit *one-dimensional* electron

transport [4, 5]. The correct atomic arrangement is also critical for understanding the charge density distribution and in turn the surface electronic structure that is relevant, for example, to the development of nanocatalysts [6]. Improving efficiency and selectivity of catalysts will have significant economic benefit for the chemical industry. DFT has also been used to design electrode materials for lithium ion batteries. For example, Meng et al. have correlated structure with performance in electrodes using ab initio methods [7]. Materials design for batteries is crucial for development of plug-in electric vehicles that meet consumer performance requirements. Overall DFT allows for fundamental understanding of the relationship between atomic structure and electronic structure that is critical for understanding and utilizing physical properties of nanoscale systems.

Measurement Techniques

Photoelectron Spectroscopy

Photoelectron spectroscopy (PES) is a traditional surface analysis technique that uses a photon beam to provide energy for electrons to escape the potential of atoms or molecules near the surface. Kinetic energy distributions of emitted photoelectrons provide information regarding ionization energies or work function of the surface that reflects the composition and electronic states on the surface. Typical methods are x-ray photoelectron spectroscopy (XPS) that uses soft X-rays with energy on the order of 200–2,000 eV and ultraviolet photoelectron spectroscopy (UPS) that uses ultraviolet light with energy in the range of 10–45 eV. The energy of the photon beam affects the type of electrons that are emitted from the sample. During XPS core electrons are emitted from the atoms and during UPS the energy is sufficient to emit only valence electrons. Angle resolved photoemission spectroscopy (ARPES) provides additional information about the momentum of the emitted electrons. Since momentum is conserved, one can obtain the energy-momentum relationship (called the dispersion relationship) of the electrons in the crystal that reflects the energy band structure as a function of crystallographic direction. ARPES has been an important tool to measure the electronic band structure in bulk materials and in quantum-confined systems. For example, Yeom et al. measured a charge density wave in linear chains of indium atoms on silicon (001) surfaces [8]. Charge density waves are a coupling between electrons and lattice vibrations that exhibit a periodic modulation of charge that can be observed on a *one-dimensional* metallic surface. In the same study, a measured temperature dependent metal to semiconductor transition for in atomic chains on silicon (001) was attributed to a Peierls transition that is another signature of *one-dimensional* quantum confinement.

Scanning Probe Microscopy

Scanning probe microscopy (SPM) includes techniques such as scanning tunneling microscopy/spectroscopy (STM/STS), atomic force microscopy (AFM), electrostatic force microscopy (EFM), and Kelvin probe force microscopy (KPFM) that can be used to measure atomic structure and/or surface electronic structure. STM, invented in 1981 by Binnig and Rohrer, probes both atomic and electronic structure on surfaces by measuring tunneling current from the probe tip to sample surface across a narrow vacuum (dielectric) gap. STM measurements typically achieve atomic scale spatial resolution. The AFM was invented shortly after the STM, 1986, to measure topography on nonconducting surfaces and is also capable of atomic and molecular resolution on surfaces. AFM measures van der Waals and electrostatic forces between cantilever tip and surface and thus does not require a conductive sample surface. KPFM is a variant of AFM in which conducting tips are used; KPFM allows for determination of the local surface potential with nanometer spatial resolution.

Tunneling current, as measured in STM, is extremely sensitive to both electron density and surface topography and convolutes the two properties. The tip-sample polarity affects whether electrons tunnel from sample to tip or from tip to sample and thus determines if the measurement probes filled or empty surface electronic states, respectively. A combination or empty and filled states imaging is often used in order to deconvolute the surface electronic structure from the atomic structure. STM can resolve corrugations heights on the sub-angstrom level, i.e., 0.2 Å corrugations between atoms on a clean platinum surface have been measured. The atomic arrangement on clean Pt (111) and how the surface structure evolves after depositing self-assembled monolayers on the surface have been measured using STM [9]. Figure 3a shows an STM image of Pt(111) where the hexagonal close

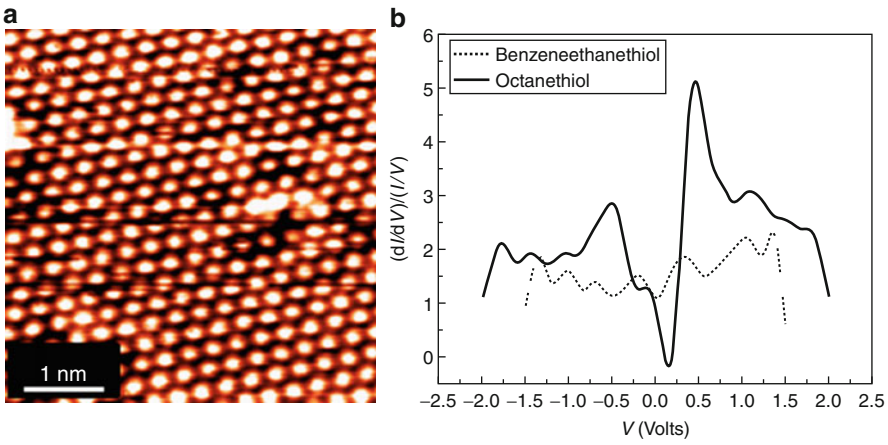

Surface Electronic Structure, Fig. 3 (**a**) STM image of Pt(111) surface. *R. Ragan unpublished results* (**b**) Normalized differential conductance of self-assembled monolayers of benzenethiol (*dashed curve*) and octanethiol (*solid curve*) on Pt(111) (Printed with permission from Ref. [10])

packing of the atoms on the surface is easily observed. Scanning tunneling spectroscopy (STS) is a derivative of STM that measures the density of electronic states in the vicinity of the atomic scale STM tip, again yielding high spatial resolution. During STS, the current–voltage spectrum is measured between tip and surface while the voltage is swept across a specified range usually at constant tip-to-sample distance. Normalization of the differential conductance (dI/dV) with the conductance (I/V) can reflect the local density of states near the Fermi energy. Figure 3b shows normalized differential conductance data for benzene ethanethiol and octanethiol self-assembled monolayers on Pt(111) determined from STS data. Note that the Fermi energy is set at zero volts on the x-axis. The octanethiol/Pt(111) junction has zero conductance at the Fermi energy and this represents an energy bandgap, i.e., no available states near the Fermi energy. For the benzene ethanethiol/Pt(111) junction, there is finite conductance at the Fermi energy and this is an indication of metallic behavior. A higher conductivity near the Fermi energy across benzene ethanethiol/Pt(111) junctions in comparison to octanethiol/Pt(111) junctions can be attributed to the fact that the benzene ethanethiol molecule has conjugated bonds in the molecule [9].

AFM measures the forces between AFM tip and surface by optically measuring the deflection of an AFM cantilever. With this basic mechanism, the type of signal feedback provides a wealth of information about the sample surface. Amplitude and frequency modulated AFM monitors the variation of the amplitude or frequency, respectively, of the AFM cantilever in response to forces between the tip and the surface and measures topography of the surface. In intermittent contact mode, the phase shift of the free cantilever resonance frequency provides nanometer scale information of the viscoelastic properties and adhesion force of the surface since it represents energy dissipation between tip and surface. For example, when imaging under a repulsive tip-sample condition, regions of the surface with the higher elastic modulus appears darker in a phase contrast AFM image. One can observe a contrast reversal when the tip changes from repulsive to attractive mode. Variations in local topography also induce a phase shift in the cantilever frequency and thus topography and phase images need to be analyzed in conjunction to understand the physical properties of the surface.

Derivatives of AFM can be used to measure electrical properties when using a conducting cantilever. EFM measures electrostatic forces between surface and cantilever and is modeled by treating the vacuum, air or any dielectric gap between tip and surface as a capacitor. The force is dependent on the tip-surface distance and the potential difference between tip and surface. In particular, KPFM directly measures the contact potential difference (difference between sample surface work function and tip work function) using a lock-in technique to null the electrostatic forces between tip and sample surface. Recently, Ragan and Wu et al. have demonstrated that measured values of work function obtained from KPFM compare quantitatively with DFT calculations and together provide information on the atomic arrangement and termination of atoms on alloy surfaces [6]. Work function variations on surfaces reflect charge transfer [11, 12], quantum-size effects [13], and localized surface

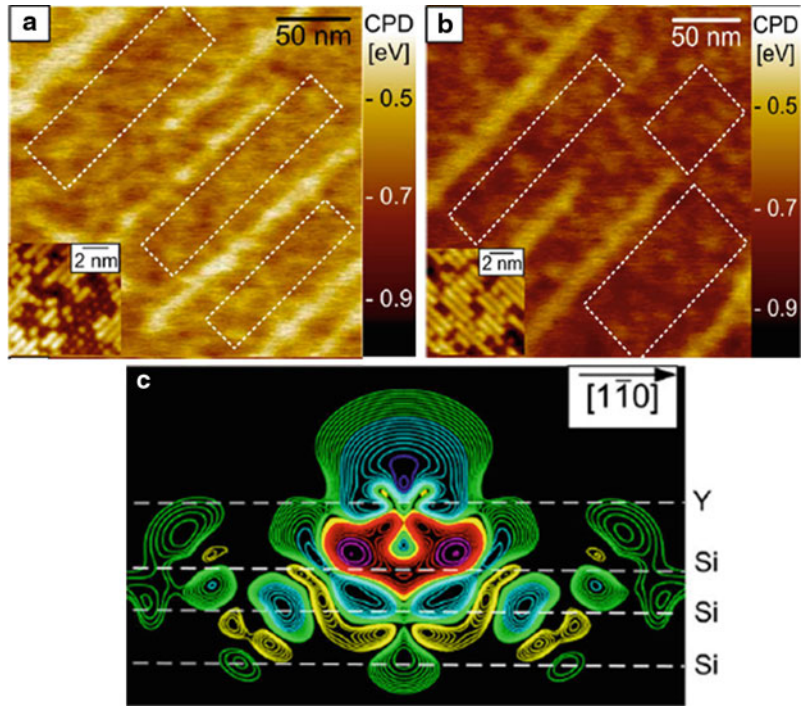

Surface Electronic Structure, Fig. 4 KPFM images of dysprosium nanowires on Si(001) that have been annealed post-growth at (**a**) 600°C and (**b**) 680°C. (**c**) Simulated charge density difference image for a single metal adatom on Si(001) with the cross section perpendicular to the surface. Charge accumulation increases from yellow to pink contour lines, whereas charge depletion increases from green to blue contour lines. The greatest charge depletion is seen at the metal adatom location and the greatest charge accumulation is seen in the region between the adatom and the subsurface Si atoms (Printed with permission from Ref. [11])

charge [14]. Figure 4 demonstrates how the work function on silicon changes when metal adatoms are on the semiconductor surface due to charge transfer between metal adatoms and substrate atoms. Figure 4a is a KPFM image after deposition of dysprosium on Si(001) and annealing the sample at 600°C. Metallic disilicide nanowires form on the surface and appear as bright lines in the KPFM image since the disilicide nanowires have a lower work function than the Si(001) substrate. The Si(001) substrate in between nanowires is highlighted with white dashed boxes. A comparison of the substrate regions in Fig. 4a with those in Fig. 4b shows that the work function is lower on the substrate regions of the former. The STM images shown as insets in the lower left corner show that the Si(001) surface in Fig. 4a has more metal adatoms (dark regions in STM image) on the surface than the Si(001) surface of Fig. 4b due to the lower annealing temperature. The DFT simulation of Fig. 4c demonstrates that metal adatoms transfer charge to the Si atoms on the surface. This creates a dipole on the surface that lowers the work function [11]. Overall, KPFM measurements provide information about material behavior in devices; KPFM across heterojunctions provides information regarding band offsets, device performance of diodes and chemical sensitive field effect transistors and trapped charge at interfaces in high electron mobility transistors.

Ion Scattering

Low energy ion scattering (LEIS) is a method complimentary to scanning probe techniques that also provides information about surface composition, electronic structure, and atomic structure. LEIS has less stringent requirements on surface conditions than SPM as data can be acquired using LEIS from rough and contaminated materials. The energy of scattered ions depends on the ratio of the projectile and target masses, providing a measure of the atomic mass distribution on the surface. The degree of charge exchange that occurs during scattering is dependent on the surface electronic properties when using projectiles with low ionization energies, such as alkalis. When an alkali-metal atomic particle is in the vicinity of a surface, its ionization level shifts up due to the image charge interaction, while it broadens due to overlap of the ion and surface wave functions. The measured neutral fraction depends on the ionization potential, the degree that the level shifts near the surface, and the work function at a point just above the scattering site. The charge

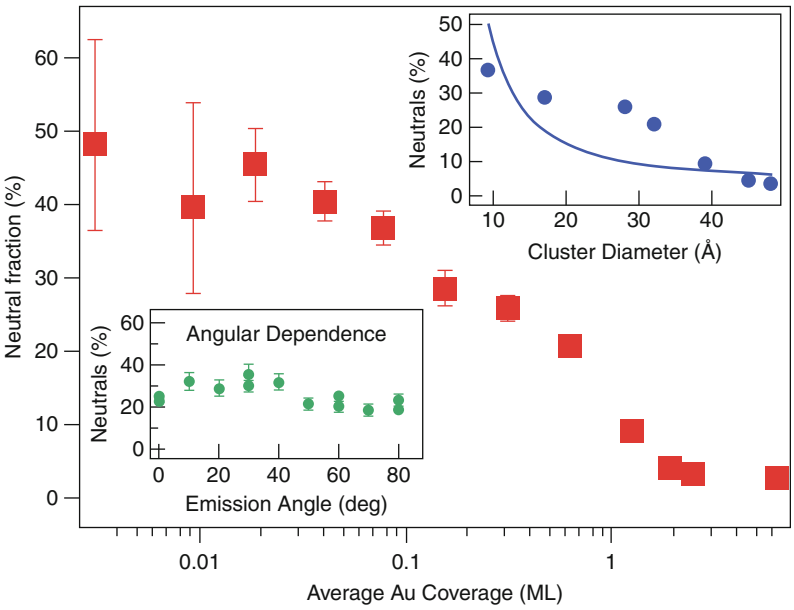

Surface Electronic Structure, Fig. 5 Neutral fractions (NF) of singly scattered 2.0 keV Na ions shown sas a function of the average Au coverage. The right side inset shows NF versus cluster diameter, with the symbols indicating experimental data and the solid line a theoretical fit. The left side inset shows NF for Na+ scattered from a 0.15 ML Au coverage as a function of the emission angle with respect to the surface normal (Printed with permission from Ref. [16])

exchange process is well described by a non-adiabatic resonant charge transfer model [15]. Since the interaction is local to the site where projectile atoms exit the surface, the neutralization of low energy alkali ions provides a unique method for measuring the local work function and quantum-size behavior in nanomaterials.

Yarmoff et al. has used LEIS to measure quantum-size effects in the electronic structure of gold nanoclusters on TiO_2 [16] to provide insight regarding how catalytic activity and surface electronic structure are correlated. Au or other heavy metal nanocrystals are ideal for ion scattering experiments, as the large mass of the cluster atoms enables a complete separation of the ions that impact the nanoclusters from those that impact the substrate. The integrated single scattering peaks in "Neutrals" and "Total Yield" spectra are divided to obtain the neutral fraction for scattering from the clusters. The neutral fraction for Na^+ ions scattered from Au nanocrystals as a function of Au coverage is directly correlated with the size of the Au nanocrystals. The neutral fraction goes from about 50% for the smallest clusters down to about 3% for the film [16]. The enhanced neutralization from small clusters is due to participation of quantum-confined states in the non-adiabatic resonant charge transfer process. Bulk Au has a relatively high work function (5.1 eV), so that the Fermi level is degenerated with the Na ionization level (also ~5.1 eV) and most of the scattered Na remains ionic. The neutral fraction for small Au clusters is considerably larger than for bulk Au because filled states associated with the clusters provide electrons that can tunnel to the outgoing projectile. The existence of such filled states is consistent with reports that small Au clusters are negatively charged. The additional filled states above the Fermi level depend on the size of the clusters, and thus provide a measure of the quantum-size behavior (Fig. 5).

Examples of Application

Nanowire Sensors

Chemical and biological nanowire sensors that use electronic transduction are an example of a class of devices that uses changes in surface electronic structure to measure local molecular binding events or adsorption of molecules on surfaces. A chemical or biological sensor can be reduced to some basic components: a receptor (biological recognition element if selectivity is required), a transducer, and a means for processing whether or not target molecules of interest have bound to the surface and relaying this information to the user. Transducers can sense molecular interactions electronically (e.g., changes in localized charge) or optically (e.g., changes in dielectric constant). Changes in surface electronic structure can affect the conductance and this is easily measured in an electronic platform. A high surface to volume ratio in nanowires leads to high sensitivity for measuring

changes in conductance due to surface binding events. If the surface of nanowires is functionalized with receptors that selectively bind to the target molecule of interest then selectivity can be engineered into the sensor platform. Since an early demonstration of semiconducting carbon nanotubes as chemical sensors, many different materials that form nanowires have exhibited the capability to sense molecules. In_2O_3 nanowires, SnO_2 nanoribbons, Si and ZnO nanowires have all been used as chemical and/or biological sensors. Si nanowires have been used for the detection of DNA hybridization, protein–protein interactions, cancer markers, and viruses. Some recent review articles that discuss nanowires-based sensor devices are referenced here [17, 18].

Nanowire sensors based on electronic transduction are commonly fabricated in a field effect transistor (FET) architecture with a back gate configuration. A single or multiple nanowires are connected to a source and drain and nanowires serve as the conducting channel. The conductance in the channel will change as molecules bind to the surface. Molecular binding events on semiconducting nanowire surfaces induce accumulation (depletion) of charge carriers that can be measured as an increase (decrease) lateral conductivity along nanowires in the FET architecture. The onset of accumulation or depletion of carriers depends on the surface charge induced and the carrier-type in the nanowire, *n-type* signifies that the majority carriers are negatively charged electrons and *p-type* signifies that the majority carriers are positively charged holes. Thus in a FET architecture, molecular binding events on surfaces can be monitored in an electronic circuit. For example, in a study by Cui et al. Si nanowires were functionalized with biotin receptors. When streptavidin, target molecule, was introduced into the system at a concentration of 250 nM an increase in conductance was observed. Streptavidin is well known to have a high binding affinity with biotin. The increase in conductance due to the introduction of strepavidin could be measured for concentrations as low as 25 pM [17, 18]. This early study demonstrated both selectivity and high sensitivity of Si nanowire sensors.

Si has some advantages as a sensing platform since microelectronic circuits are typically made from Si. This approach provides a strategy for fabricating high-density, high-quality nanoscale sensors that can be integrated with Si-based circuits. Si nanowire sensors have been fabricated by either "top-down" or "bottom-up" fabrication methods where the former uses lithographic methods and the latter uses self-organization routes. Previously, Li et al. reported an approach to configure FET device architectures using Si nanowires for DNA sensors using a standard "top-down" semiconductor process [19]. Reactive ion etching is used to fabricate Si nanowires on silicon-on-insulator substrates that have been patterned using electron beam lithography. Figure 6a is an optical image of the entire sensor system. Figure 6b, c are high-resolution SEM images showing a Si nanowire in the system. The chemical functionalization process to bind a single strand DNA receptors on nanowire surfaces is illustrated in the schematic of Fig. 6d. The chemical modification process can be monitored after each step by measuring changes in surface potential using the surface photovoltage technique. When solutions containing complementary strands of DNA with concentrations of 25 pmol are introduced to *p-type* Si nanowire surfaces, there is an increase in conductance due to accumulation of carriers. In the case of *n-type* Si nanowires, the DNA binding event leads to a decrease in conductance due to depletion of carriers. Accumulation (*p-type*) or depletion (*n-type*) of carriers is associated with the negative charge on the backbone of DNA molecules. Quitoriano et al. introduced a different fabrication method for Si nanowire FET devices. This method is a combined "bottom-up" and "top-down" fabrication process utilizing the vapor-liquid–solid growth mechanism and optical lithography to fabricate FET devices [20, 21]. In this method, Au nanoparticles are deposited on the bottom surfaces of lithographically defined Si electrodes that overhang over a recessed trench of silicon dioxide. The growth of Si nanowires is guided from the bottom of the electrode at the site of the Au catalyst along the silicon dioxide layer to the opposite electrode. A benefit of combining "bottom-up" methods with "top-down" methods is to integrate nanowires into microelectronic circuits using high-throughput methods. In both cases, Si nanowires sensors can be connected directly to the adjoining circuitry for signal amplification and automated data acquisition.

Nanoscale Catalysts

Metallic and bimetallic surfaces and nanostructures with tunable physical and chemical properties have attracted particular attention in recent years due to

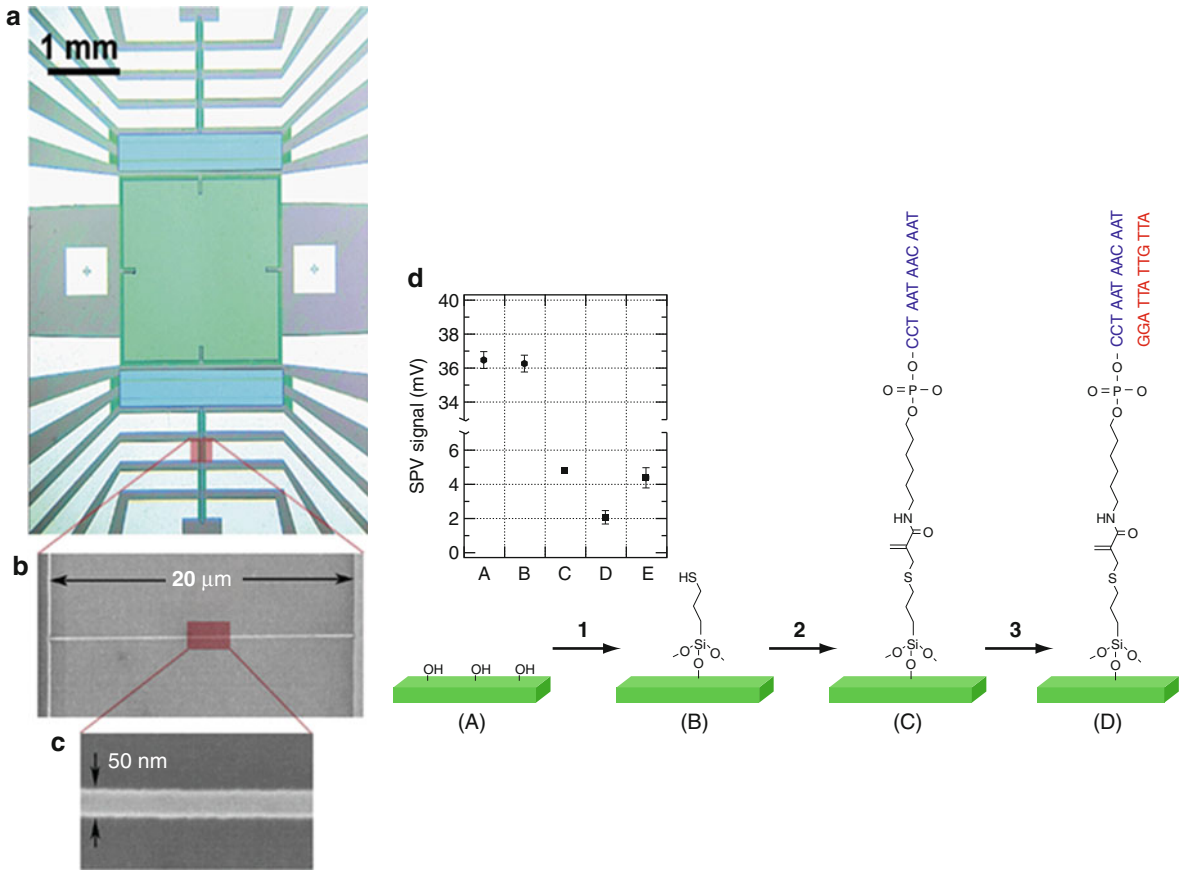

Surface Electronic Structure, Fig. 6 (**a**) Optical image of lab on chip system using Si nanowires for signal transduction. (**b**) SEM image of Si nanowire spanning electrical leads. (**c**) High-resolution SEM image of Si nanowire. (**d**) Chemical functionalization of Si nanowire surfaces, steps labeled A-D, for sequence specific detection of DNA. The inset shows how the change in surface photovoltage (SPV) signal monitors each chemical functionalization step. (Printed with permission from Ref. [19])

their potential for use in a broad range of applications. The discovery by Haruta, et al. that gold nanoparticles on oxide supports exhibit surprisingly high catalytic activity for reactions such as CO oxidation and propylene epoxidation has inspired an enormous wave of research in the quest for innovative nanocatalysts. Chemically active Au nanoparticles have been prepared on reducible (TiO_2, ZrO_2, NiO, or Fe_2O_3) oxides, and irreducible (SiO_2 or Al_2O_3) oxides in order to gain insight on the role of quantum-size effects, facets and steps at the edges of nanoclusters, and charge transfer to the substrate in chemical activity. A review of mechanisms involved in enhanced activity of Au nanoclusters can be found here [22]. Bimetallic surfaces of Pt and Pd, and trimetallic nanoparticles of Au/Pt/Rh were also found to be highly effective in promoting a variety of reactions, typically higher than corresponding monometallic nanoparticles. Thus there appears to be a variety of parameters affecting chemical activity.

Surface electronic structure has been identified as playing an important role in enhanced catalytic activity in nanoscale metallic systems. Electronic structure can be modified in nanosystems in many ways such as by charge transfer between nanocatalyst and substrate support or due to alloy effects in bimetallic systems. Both experimental and theoretical results show the strong coupling between electronic structure and catalytic activity. The Hammer-Nørskov model predicted that chemisorption energy correlates with the d-band center in transition metals and this is experimentally observed for oxygen and sulfur chemisorption energies

on different metal surfaces [23]. The effect of electronic structure and its relationship to catalytic activity is also observed in experiments. For example, Au clusters on TiO_2 were measured by STS to undergo a metal to insulator transition at nanometer length scales. The nanocluster size were the metal to insulator transition occurs exhibited the highest turnover frequency for CO oxidation, while larger clusters having no band gap had lower activity [24]. It has also been shown that catalytic reaction rates, in the context of electrochemical catalysis, exhibit an exponential dependence on the catalyst work function and catalytic rate enhancements of up to a factor of 60 having been reported. Changes in work function as small as 200 meV can lead to an increase in rate enhancement by a factor of 10 [25]. The work function of Au nanowires can be varied by surface alloying [6] in order to optimize catalytic properties. Heterogeneous metal nanocatalysts with clusters that are a few nanometers in size hold great promise because of their large surface area to volume ratios, the availability of an enormous number of active sites and their enhanced resistance to poisoning from products of the reactions.

Cross-References

- ▶ Ab initio DFT Simulations of Nanostructures
- ▶ Atomic Force Microscopy
- ▶ Kelvin Probe Force Microscopy
- ▶ Nanomaterials for Electrical Energy Storage Devices
- ▶ Nanostructure Field Effect Transistor Biosensors
- ▶ Scanning Tunneling Microscopy
- ▶ Scanning Tunneling Spectroscopy
- ▶ Self-assembly

References

1. Wildoer, J.W.G., Venema, L.C., Rinzler, A.G., Smalley, R.E., Dekker, C.: Electronic structure of atomically resolved carbon nanotubes. Nature **391**, 59 (1998)
2. Berger, C., Song, Z.M., Li, T.B., Li, X.B., Ogbazghi, A.Y., Feng, R., Dai, Z.T., Marchenkov, A.N., Conrad, E.H., First, P.N., de Heer, W.A.: Ultrathin epitaxial graphite: 2D electron gas properties and a route toward graphene-based nanoelectronics. J. Phys. Chem. B **108**, 19912 (2004)
3. Freeman, A.J., Wu, R.Q.: Electronic-structure theory of surface, interface and thin-film magnetism. J. Magn. Magn. Mater. **100**, 497 (1991)
4. Shinde, A., Wu, R., Ragan, R.: Thermodynamic driving forces governing assembly of disilicide nanowires. Surf. Sci. **604**, 1481 (2010)
5. Zeng, C., Kent, P.R.C., Kim, T., Li, A., Weitering, H.H.: Charge-order fluctuations in one-dimensional silicides. Nat. Mater. **7**, 539 (2008)
6. Ouyang, W., Shinde, A., Zhang, Y., Cao, J., Ragan, R., Wu, R.: Structural and chemical properties of gold rare earth disilicide core – shell nanowires. ACS Nano **5**, 477 (2011)
7. Meng, Y.S., Arroyo-de Dompablo, M.E.: First principles computational materials design for energy storage materials in lithium ion batteries. Energy Environ. Sci. **2**, 589 (2009)
8. Yeom, H.W., Takeda, S., Rotenberg, E., Matsuda, I., Horikoshi, K., Schaefer, J., Lee, C.M., Kevan, S.D., Ohta, T., Nagao, T., Hasegawa, S.: Instability and charge density wave of metallic quantum chains on a silicon surface. Phys. Rev. Lett. **82**, 4898 (1999)
9. Ragan, R., Ohlberg, D., Blackstock, J.J., Kim, S., Williams, R.S.: Atomic surface structure of UHV-prepared template- stripped platinum and single-crystal platinum (111). J. Phys. Chem. B **108**, 20187 (2004)
10. Lee, S., Park, J., Ragan, R., Kim, S., Lee, Z., Lim, D.K., Ohlberg, D.A.A., Williams, R.S.: Self-assembled monolayers on Pt(111): molecular packing structure and strain effects observed by scanning tunneling microscopy. J. Am. Chem. Soc. **128**, 5745 (2006)
11. Shinde, A., Cao, J.X., Lee, S.Y., Wu, R.Q., Ragan, R.: An atomistic view of structural and electronic properties of rare earth ensembles on Si(001) substrates. Chem. Phys. Lett. **466**, 159 (2008)
12. He, T., Ding, H.J., Peor, N., Lu, M., Corley, D.A., Chen, B., Ofir, Y., Gao, Y.L., Yitzchaik, S., Tour, J.M.: Silicon/molecule interfacial electronic modifications. J. Am. Chem. Soc. **130**, 1699 (2008)
13. Lee, S., Shinde, A., Ragan, R.: Morphological work function dependence of rare-earth disilicide metal nanostructures. Nanotechnology **20**, 6 (2009)
14. Rosenwaks, Y., Shikler, R., Glatzel, T., Sadewasser, S.: Kelvin probe force microscopy of semiconductor surface defects. Phys. Rev. B **70**, 085320 (2004)
15. Kimmel, G.A., Goodstein, D.M., Levine, Z.H., Cooper, B.H.: Local adsorbate-induced effects on dynamic charge-transfer in ion-surface interactions. Phys. Rev. B **43**, 9403 (1991)
16. Liu, G.F., Sroubek, Z., Yarmoff, J.A.: Detection of quantum confined states in Au nanoclusters by alkali ion scattering. Phys. Rev. Lett. **92**, 216801 (2004)
17. Patolsky, F., Lieber, C.M.: Nanowire nanosensor. Mater. Today **8**, 20 (2005)
18. Kolmakov, A., Moskovits, M.: Chemical sensing and catalysis by one-dimensional metal-oxide nanostructures. Annu. Rev.Mater. Res. **34**, 152 (2005)
19. Li, Z., Chen, Y., Li, X., Kamins, T.I., Nauka, K., Williams, R.S.: Sequence-specific label-free DNA sensors based on silicon nanowires. Nano Lett. **4**, 245 (2004)
20. Quitoriano, N.J., Kamins, T.I.: Integratable nanowire transistors. Nano Lett. **8**, 4410 (2008)
21. Quitoriano, N.J., Wu, W., Kamins, T.I.: Guiding vapor-liquid-solid nanowire growth using SiO_2. Nanotechnology **20**, 145303 (2009)

22. Min, B.K., Friend, C.M.: Heterogeneous gold-based catalysis for green chemistry: low-temperature CO oxidation and propene oxidation. Chem. Rev. **107**, 2709 (2007)
23. Greeley, J., Norskov, J.K., Mavrikakis, M.: Electronic structure and catalysis on metal surfaces. Annu. Rev. Phys. Chem. **53**, 319 (2002)
24. Valden, M., Lai, X., Goodman, D.W.: Onset of catalytic activity of gold clusters on titania with the appearance of nonmetallic properties. Science **281**, 1647 (1998)
25. Vayenas, C.G., Bebelis, S., Ladas, S.: Dependence of catalytic rates on catalyst work function. Nature **343**, 625 (1990)